Preferential concentration of heavy particles in a turbulent channel flow

John R. Fessler, Jonathan D. Kulick, and John K. Eaton

Citation: Phys. Fluids **6**, 3742 (1994); doi: 10.1063/1.868445
View online: http://dx.doi.org/10.1063/1.868445
View Table of Contents: http://pof.aip.org/resource/1/PHFLE6/v6/i11
Published by the American Institute of Physics.

Preferential concentration of heavy particles in a turbulent channel flow

John R. Fessler, Jonathan D. Kulick, and John K. Eaton
Department of Mechanical Engineering, Stanford University, Stanford, California 94305

(Received 5 October 1993; accepted 6 July 1994)

An investigation of the instantaneous particle concentration at the centerline of a turbulent channel flow has been conducted. The concentration field was obtained by digitizing photographs of particles illuminated by a spanwise laser sheet and identifying individual particles. The resulting distribution was then compared to the expected distribution for the same number of particles randomly distributed throughout the volume. Significant departures from randomness have been found and the differences are strongly dependent on the time constants of the particles. Five different particle classes were investigated and the maximum departure from randomness was found when the ratio of the particle's aerodynamic response time to the Kolmogorov time scale of the flow was approximately one. The length scales of the particle clusters were found to change with the particle size. The correlation dimension was used to produce a single parameter describing the degree of concentration regardless of the scale on which it occurs. The spacing between particle clusters was also investigated and found to be much larger than the scales on which concentration occurs.

I. INTRODUCTION

The mixing and diffusion of particles by turbulence is of interest for applications ranging from electrostatic precipitation of solid particulates to the atmospheric transport of pollutants. Traditionally, particle dispersion has been treated in a statistical sense by assuming a Fickian diffusion process in which particles diffuse from regions of high mean concentration to low mean concentration. A diffusion type analysis can only treat the particle number density field in a time-averaged sense and its use implies that particles which are initially uniformly distributed will remain uniformly distributed. The diffusion model, however, misrepresents the true physics of the situation. Such modeling implicitly assumes that the turbulence is purely stochastic and that the fluctuating drag on the particle causes it to undergo a random walk. It is now well known that turbulence is usually dominated by semi-organized or coherent structures. Such structures would be expected to move particles in an organized manner and are likely to produce instantaneous concentration fluctuations even if the particles are initially uniformly distributed. In certain situations the response of the particles to the coherent structures may lead to a complete breakdown of the diffusion model and result in such phenomena as countergradient diffusion.

The degree to which turbulent eddies can modify the instantaneous concentration field depends on the Stokes number (Crowe *et al.*[1]) defined as the ratio of the particle aerodynamic response time, τ_p, to some representative time scale in the flow, τ_f:

$$\mathrm{St} \equiv \frac{\tau_p}{\tau_f}. \tag{1}$$

Particles with very small Stokes numbers will simply be flow tracers so if the fluid is well mixed by turbulence these particles should be randomly distributed. Very large Stokes number particles, on the other hand, will not have sufficient time in a fluid element to respond to fluctuations in its velocity and will simply pass unaffected through any turbulence structure. Particles with Stokes numbers on the order of one will respond somewhat to the turbulent motions but cannot follow tightly curved streamlines. The instantaneous concentration field may therefore be modified in the vicinity of turbulent eddies.

Eaton and Fessler[2] reviewed studies of dilute, particle laden gas flows which include measurements of the instantaneous concentration field. Most of the previous studies examined simple free shear flows which are dominated by large-scale, two-dimensional or axisymmetric vortices (cf. Kobayashi *et al.*,[3] Wen *et al.*,[4] Lazaro and Lasheras,[5,6] Yang *et al.*,[7] and Longmire and Eaton[8]). All of these researchers have observed highly organized particle concentration fields for Stokes numbers on the order of one. Particles were flung away from the vortex cores and in many cases collect in rings surrounding the vortices. In the jet and wake flows the particles are concentrated in the highly strained saddle region between successive vortices.

Less work has been done on examining the particle concentration field in flows with fully three dimensional turbulence structures. The concentration field in wall-bounded flows has been examined in water-flow experiments (e.g., Rashidi *et al.*,[9] Young and Hanratty[10]) and in numerical simulations (Brooke *et al.*,[11] Pedinotti *et al.*,[12] Rouson and Eaton[13]). All of these studies have focused on the very near wall region where the dominant effect is the collection of particles into the low speed streaks. Analytical and numerical simulations have shown that preferential concentration of particles into specific turbulence structures can also occur in homogeneous flows. Maxey[14] used asymptotic methods to show that particles should be concentrated in regions of low vorticity and high strain rate. Squires and Eaton[15,16] confirmed this result using direct numerical simulations of homogeneous, isotropic turbulence. They found local concentrations up to 30 times the mean. They classified their flow into four types of zones and found high mean concentrations in convergence zones and low concentrations in eddies.

 1070-6631/94/6(11)/3742/8/$6.00

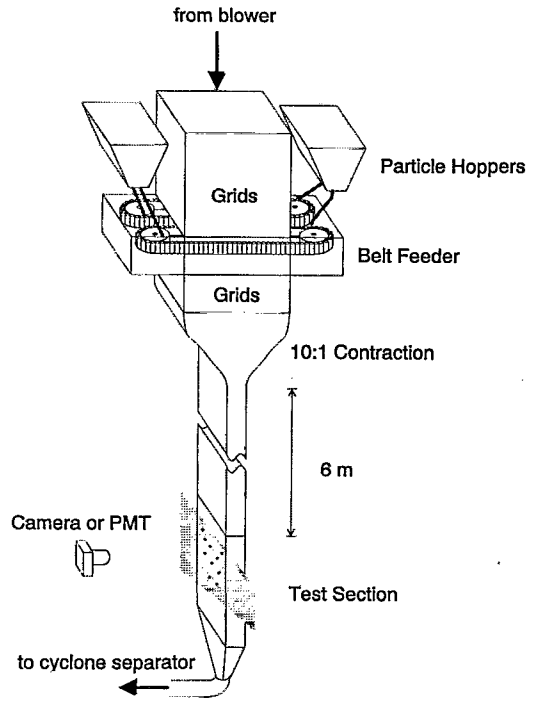

FIG. 1. Schematic of fully developed channel flow facility.

Wang and Maxey[17] also used direct numerical simulation of isotropic turbulence and found that the particles were most strongly concentrated when the Stokes number based on the Kolmogorov time scale was about one. The results of both of the aforementioned numerical studies have been called into question with some believing that the preferential concentration is an artifact of the artificial forcing schemes used to maintain stationarity in the simulations. Neumann and Umhauer[18] experimentally investigated the spatial separation distribution of nearest neighboring particles in a vertical down-flowing pipe. They found that this distribution was significantly different from what one would expect for particles distributed purely at random. The distribution was shifted toward smaller separation distances, implying that the particles are much more closely packed in some regions.

The current study investigates the instantaneous particle concentration field at the centerline of a fully developed turbulent channel flow. A spanwise cut at the centerline represents a region of nearly homogeneous flow as there are no streamwise gradients, a large aspect ratio insures no spanwise gradients and gradients in the normal direction are zero by symmetry. This region provides an ideal situation for observing particle response to small scale turbulent motions.

II. EXPERIMENTAL FACILITY

The experiments were conducted in a fully developed turbulent channel of aspect ratio 11.4:1. The flow is downward eliminating any concentration gradients due to gravity. The channel half-width is 2 cm with 6 m of flow development prior to the test section, yielding 300 half-widths of development length. The tunnel was operated at a centerline velocity of 10.5 m/s giving a Reynolds number based on channel half-width of 13,800. Figure 1 shows a schematic of the wind tunnel apparatus and Table I gives a summary of the relevant parameters of the channel flow. Estimates of the dissipation and Kolmogorov length scale were taken from a $k-\epsilon$ computation of a turbulent channel flow at Re=13 800 by Sato.[19] Further details on the experimental facility are given in Kulick *et al.*[20]

Five different particles were used in the study giving a range of Stokes numbers from 0.74 to 41. Table II summarizes the physical characteristics of the particles. Note that Table II gives two values for the time constant, τ_p, for each of the particles, one assuming ideal Stokes flow and a corrected value. Correction to the Stokes τ_p was made using an empirical relationship as cited in Torobin and Gauvin[21] for $\mathrm{Re}_p \leqslant 700$,

$$C_D = \frac{24}{\mathrm{Re}_p}[1+0.15\ \mathrm{Re}_p^{0.687}]. \tag{2}$$

The Stokes numbers given in Table II, St_k, are based on the corrected τ_p and the Kolmogorov time scale, $\tau_f=(\nu/\epsilon)^{1/2}$. The particles are loaded in the flow conditioning section of the tunnel, prior to a 10:1 contraction. The 50 μm glass, 90 μm glass, and 70 μm copper particles are loaded with a system of small aluminum buckets glued to two timing belts. The buckets are filled rapidly from pressurized hoppers and then dragged through the flow conditioning section where they drain slowly. This device allows variation of the particle mass loading simply by varying the speed of the belts. A section containing two grids, a screen, a contraction, and a honeycomb at the exit of the contraction insures that the flow enters the development section with uniform particle concentration. The 25 μm glass and 28 μm Lycopodium were introduced through a pressurized bottle draining into the flow conditioning section. As these particles were introduced earlier in the tunnel they passed through four additional grids which served to enhance dispersion of the particles. The mass loading ϕ, defined as the ratio of the mass flow of particles to the mass flow of air, was varied for each of the particles to provide a consistent number density. Consistent mass loadings were not feasible owing to the nature of the measurement technique and the wide range of particle sizes and densities.

III. EXPERIMENTAL PROCEDURE

A. Concentration field measurements

All data for determining the particle concentration field were taken from photographs of particles illuminated by a

TABLE I. Channel flow parameters.

Channel half-width, h	20 mm
U_{cl}	10.5 m/s
Re_h	13 800
U_τ	0.49 m/s
Viscous length scale	31 μm
ϵ, centerline (est.)	2.8 $\mathrm{m}^2/\mathrm{s}^3$
η, centerline (est.)	190 μm
Kolmogorov time scale, $(\nu/\epsilon)^{1/2}$	2.3 ms

TABLE II. Particle parameters.

Nominal diameter	28 μm	25 μm	50 μm	90 μm	70 μm
Material	Lycopodium	glass	glass	glass	copper
Standard deviation of diameter	···	···	3.1 μm	4.5 μm	10.9 μm
Density (kg/m^3)	700	2500	2500	2500	8800
Mass loading, ϕ	3%	3%	40%	40%	100%
Stokes τ_p (ms)	1.7	5	19	63	130
Corrected τ_p (ms)	1.7	5	18	43	95
St_k	0.74	2.2	8	19	41

spanwise laser sheet long the centerline of the channel. A 10 W copper-vapor laser was passed through cylindrical optics to produce a 1 mm thick sheet at the measurement location. Each photograph represents a single 30 ns pulse from the laser and visualizes a measurement volume of approximately 3 cm by 4 cm by 1 mm. For the loadings investigated this resulted in $O(3000)$ particles per photograph.

Each photograph was enlarged and digitized on a flatbed scanner before digital processing to identify each particle's center, area and area moment of inertia (Longmire and Eaton[8]). Any particles that are close enough that their images overlap are counted as a single large particle introducing a bias against very high particle concentrations and setting an upper limit on the number densities that can be investigated. The apparent image size for an individual glass particle averages four times its true size so particles can easily appear to overlap when they are not actually agglomerated. The number densities investigated were chosen by visual inspection to be as high as possible with a minimum number of apparent overlaps. This provided well resolved statistics from a reasonable number of photographs—from 10–15 depending on the size of each image—with minimum error due to particle overlap. For this study the appropriate number density was approximately three particles per cubic millimeter.

To analyze the number density distribution, each photograph was divided into a regular grid of square boxes. Contour plots of particle concentration were produced by assigning each particle fractionally to each of its four surrounding grid points. Figure 2 shows a typical contour plot for 25 μm glass particles. This plot bears a strong resemblance to the particle number density plots of Squires and Eaton[16] for homogeneous, isotropic turbulence suggesting that the particles are preferentially concentrated. For statistical comparison, the integer number of particles per box was calculated by assigning each particle to a grid point at the center of its respective box. The distribution of number densities was then compared with what one would expect for a purely random distribution of the same average number of particles. It should be noted that particles placed randomly in a field are not uniformly distributed. Instead the number of particles in each box is a random variable that is Poisson distributed. The Poisson distribution is defined as

$$F(k)=\frac{e^{-\lambda}\lambda^k}{k!}, \tag{3}$$

where λ is the mean number of particles in each box and $F(k)$ represents the probability that an integer number of particles, k, will be found in a given box.

In order to quantify the deviation of the number density field from a completely random distribution, the following parameter, D, was calculated for each photograph:

$$D=\frac{\sigma-\sigma_{\text{Poisson}}}{\lambda}, \tag{4}$$

where σ and σ_{Poisson} represent the standard deviations for the measured particle number density distribution and the Poisson distribution, respectively, and λ is the mean particle number density. Preferential concentration of particles into clusters results in boxes with abnormally high and very low concentrations and thus large positive values of D. A uniform distribution in which every box has the same number of particles will have negative values of D and a random distribution of particles into the boxes results in D close to zero. The measured value of D must depend on the scale of the boxes used. If the box size is smaller than any turbulence scale, the distribution of particles should be random and D should be zero. Box sizes significantly larger than the largest scale in the flow, will incorporate regions of both high and

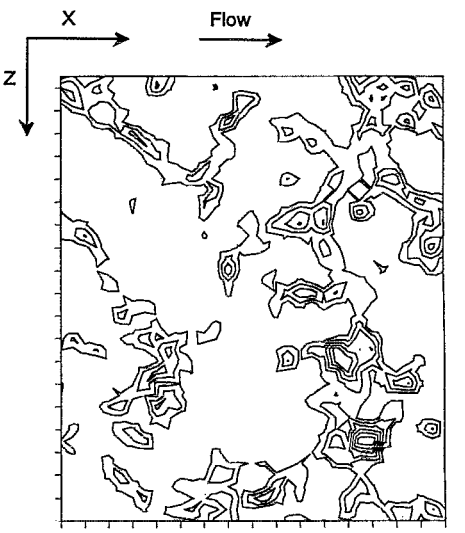

FIG. 2. Contour plot of particle number density for 25 μm glass particles with a mean concentration of 1.48. Contour levels are integer values from 2–8.

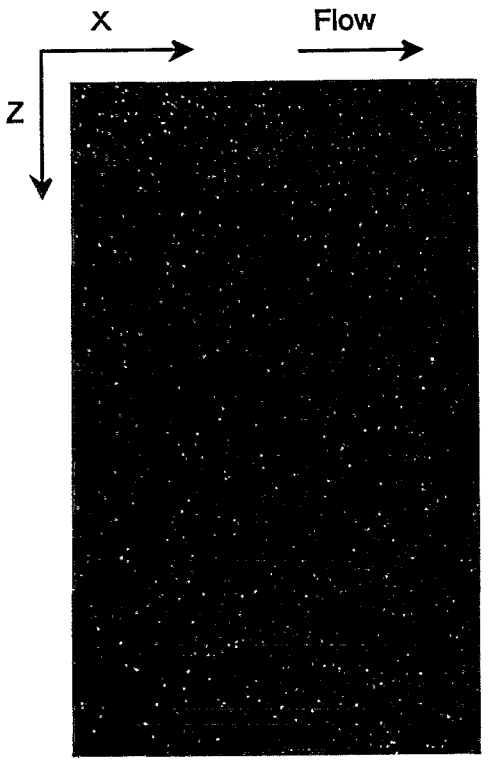

FIG. 3. Spanwise photograph of 70 μm copper particles at channel centerline. Area shown is 3 cm in streamwise direction and 4.5 cm in spanwise direction.

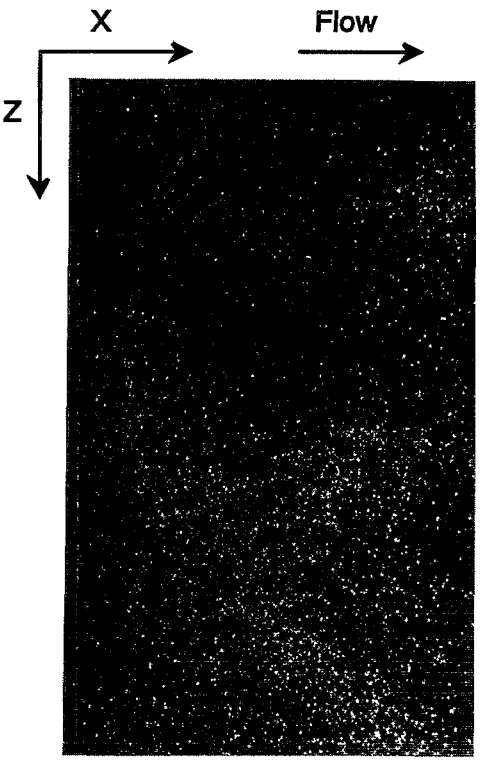

FIG. 4. Spanwise photograph of 50 μm glass particles at channel centerline. Area shown is 3 cm in streamwise direction and 4.5 cm in spanwise direction.

low concentration and again the random distribution should lead to D values of zero. It is reasonable to assume then that there will be some box size for which D is a maximum and this will provide information about the length scales on which particles are being clustered. Several box sizes from 0.5 mm to 1 cm square were used to evaluate the number density distribution for each particle class.

B. Power spectrum measurements

There are at least two length scales in the particle concentration field, one relating to the size of the particle clusters and a second relating to the spacing between clusters. The latter length scale is long relative to the size of the illuminated region so an alternative measurement was needed. Power spectra of the scattered light intensity from a fixed volume in space were measured and the length scale inferred by invoking Taylor's hypothesis. There is only an approximate relationship between the observed frequencies and actual length scales in the flow. Nevertheless, Taylor's hypothesis usually yields good estimates of streamwise length scales from velocity measurements so we might expect it to work reasonably well with the particle concentration field.

The instantaneous concentration in a 1 cubic millimeter measurement volume was obtained by measuring the intensity of light scattered from particles illuminated by a 0.5 W argon-ion laser with a 1 mm diameter beam. The laser passed along the centerline of the channel, in the same plane as the laser sheet. Receiving optics were masked and focused to observe a 1 mm square section of the beam in side scatter. A TSI photomultiplier tube that has been altered for frequency response down to 30 Hz was used to sense the scattered light intensity and a Macintosh II computer using LabView software acquired and processed the data. Spectra were taken for only the 25 and 50 μm glass particles. The spectra for 90 μm glass and 70 μm copper were dominated by low frequency behavior which the AC coupled photomultiplier tube could not resolve. The Lycopodium powder was too expensive to use for this study as only a small portion of the powder was recovered by the cyclone separator and many runs are required for smooth spectra.

IV. RESULTS

A. Particle concentration field

Figures 3–5, show representative photographs of 70 μm copper, 50 μm glass, and 28 μm Lycopodium particles, respectively. These particles represent the largest, intermediate, and smallest Stokes numbers investigated. The photographs visualize a region of the flow at the centerline of the channel that is 3 cm in the streamwise direction and 4.5 cm in the spanwise direction. It is apparent from the photographs that the copper particles are much more evenly distributed than the Lycopodium while the 50 μm glass particles are somewhere in between. Particle number density distributions for 2 mm cells are shown in Figs. 6–8, along with the Poisson distribution for the same mean particle number densities. The distributions reinforce the visual observation that the copper

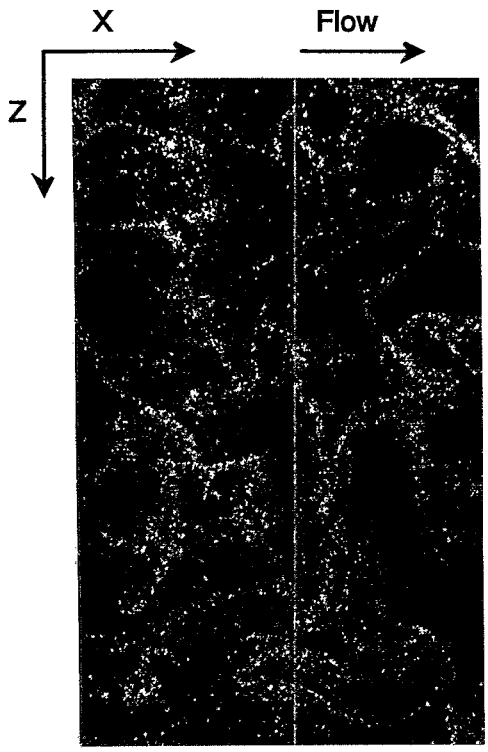

FIG. 5. Spanwise photograph of 28 μm Lycopodium particles at channel centerline. Area shown is 3 cm in streamwise direction and 4.5 cm in spanwise direction.

particles are randomly distributed while the Lycopodium particles are not. The average D parameters for these cases are 0.002, 0.268 and 0.379, respectively, which shows that D does reflect what is visually apparent.

The lack of observed preferential concentration in the case of the 70 μm copper may be somewhat misleading. It is known from Kulick *et al.*[20] that the presence of heavy particles at high mass loadings will reduce turbulence intensity in the channel flow. For example, a mass loading of 80% with 70 μm copper particles reduces the streamwise turbulence intensity, u_{rms}, by 70%. Thus at the mass loading used for this study, $\phi \approx 1$, much of the turbulence in the channel has been damped out by the particles. This introduces two explanations for the random distribution of copper particles in this study. First, the copper particles have the largest Stokes number of the particles studied, $\text{St}_k = 53$, and should be relatively unresponsive to small scale turbulent fluctuations. Second, the absence of energetic turbulent eddies due to the damping of the turbulence has removed much of the mechanism for preferentially concentrating particles. The numerical studies of Squires and Eaton[16] and Wang and Maxey[17] support the first explanation by showing decreased preferential concentration for large, heavy particles. Wang and Maxey show only one-third as much concentration for a $\text{St}_k = 2.8$ as compared to $\text{St}_k = 1.0$. Both studies used one way coupling, where the particles have no effect on the fluid field, so the Stokes number dependency was isolated from any turbulence modification. Although it is ambiguous to what degree each of the factors contributes to the lack of measured preferential concentration, the copper results do show that in the absence of a mechanism for preferential concentration,

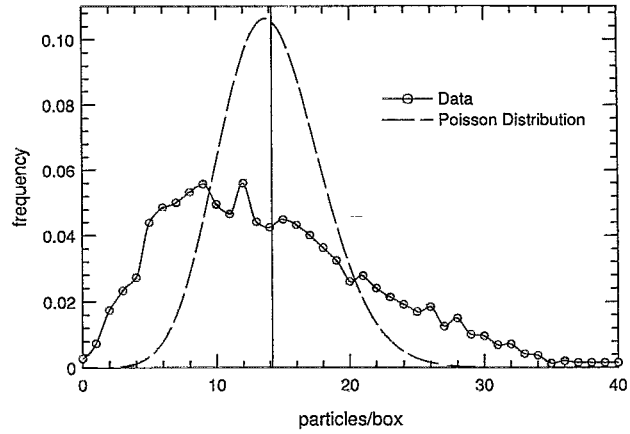

FIG. 7. Distribution of particle number density for 50 μm glass particles for 2 mm cells. Calculated from 15 photographs comprising 4073 cells.

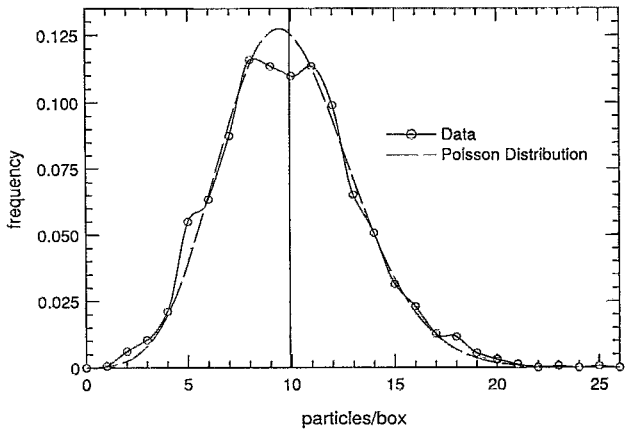

FIG. 6. Distribution of particle number density for 70 μm copper particles for 2 mm cells. Calculated from 5 photographs comprising 1658 cells.

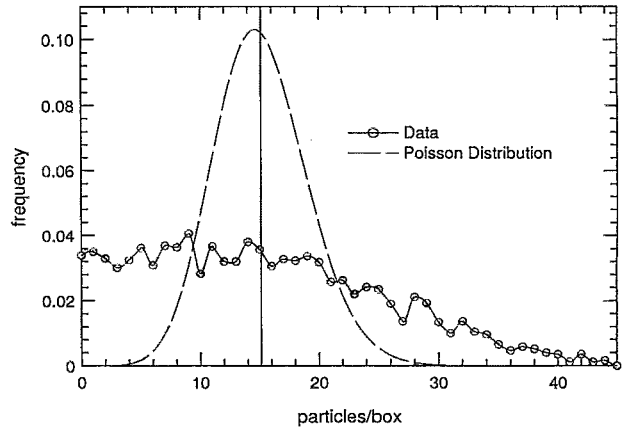

FIG. 8. Distribution of particle number density for 28 μm Lycopodium particles for 2 mm cells. Calculated from 15 photographs comprising 4316 cells.

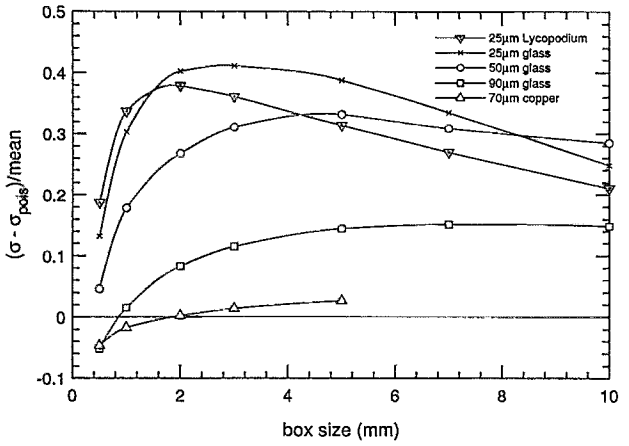

FIG. 9. Deviation of particle number density distributions from randomness for all particle sizes.

particles will be randomly distributed. This in turn validates the uniformity of the particle loading system.

Figure 9 shows a plot of D for all five particles and grid sizes ranging from 0.5 mm to 1 cm. It is interesting to note that each of the particles is randomly distributed on the scale of 0.5 mm and then, with the exception of copper, D rises to a maximum before falling off. Consideration of limiting cases supports the existence of maxima in D. At very small scales, on the order of the Kolmogorov length scale η, there are no energetic eddies available to preferentially concentrate particles. While there are energetic motions in the channel flow with large length and time scales, truly vortical motions with scales significantly greater than the channel width cannot be sustained. Thus at very small and very large scales there exists no mechanism to preferentially concentrate particles so D should be zero in these cases. As we can see that preferential concentration does occur at some scale, this necessitates at least one local maximum for D. Note also in Fig. 9 that the location of the peak in D shifts toward smaller cell sizes as the Stokes number of the particles decreases, reaching a minimum of 2 mm for the Lycopodium. This implies that the length scale on which preferential concentration occurs is a function of the particle's time constant, τ_p. This assertion seems reasonable in that small, light particles should be able to respond to smaller eddies than large, heavy particles. For length scales greater than 1 mm, the 25 μm glass particles show the greatest preferential concentration while below 1 mm the Lycopodium powder is maximally concentrated.

Figure 10 shows the maximum value of D for each of the particles plotted against their respective Stokes numbers. This plot shows the degree of preferential concentration for each particle regardless of the length scale on which it occurs. A peak is evident in this curve around a Stokes number of 2. Wang and Maxey's[17] results for homogeneous, isotropic turbulence show a strong peak in preferential concentration at $St_k=1$. Squires and Eaton looked at three particle classes with $St_k=0.325$, 0.65, and 2.27 and found the $St_k=0.65$ particles to be most preferentially concentrated in agreement with Wang and Maxey. The current experimental results indicate maximum concentration occurs at slightly higher Stokes numbers than the computational results. One explanation for this discrepancy is that the particle concentration field was evaluated using a fixed grid size in the computational studies. The grid scale for the computations was near η while the smallest grid spacing used in the experimental study is approximately 3η. We found maximum preferential concentration at $St_k=0.74$ when using a small box size of either 0.5 or 1.0 mm while maximum overall concentration was found for $St_k=2.8$ with a box size of 3 mm. This result shows that direct comparison of Fig. 10 to computational results for fixed grid spacing is inappropriate. A second possible explanation for finding peak preferential concentration at higher Stokes numbers is the wider range of scales in the experiment. The ratio of the Taylor microscale to the Kolmogorov scale, λ_T/η was approximately 20 in the experiment and $\lambda_T/\eta=10$ for the simulations of Squires and Eaton. Despite the small difference between experiment and computation, the present results support the conclusion of Wang and Maxey[17] that preferential concentration is large when the Stokes number based on the Kolmogorov time scale is near unity. It has been argued that a Stokes number based on a time scale of the large eddies is more appropriate. In fact in this flow the large eddy time scale, defined as the channel half-width divided by the centerline mean velocity, $\tau_f = h/U_{cl}$, is 2 ms as compared to 2.3 ms for τ_k so the two values are almost identical. However, as discussed in Eaton and Fessler,[2] a key mechanism in producing preferential concentration is centrifuging of particles away from vortex cores. In homogeneous turbulence, the most intense vortices occur at scales around the Kolmogorov scale (Ruetsch and Maxey[22]).

Although evaluating preferential concentration on a range of box sizes provides useful information about the scale on which preferential concentration occurs it also introduces some ambiguity about which particle is most affected by the flow. It is desirable to present a single parameter which specifies the degree of preferential concentration rather than the two numbers, D and the length scale for that value of D. Tang *et al.*[23] have used the correlation dimen-

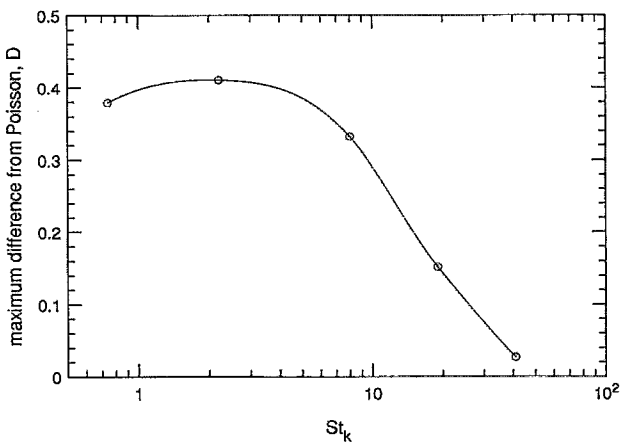

FIG. 10. Maximum deviation from randomness versus Stokes number regardless of cell size.

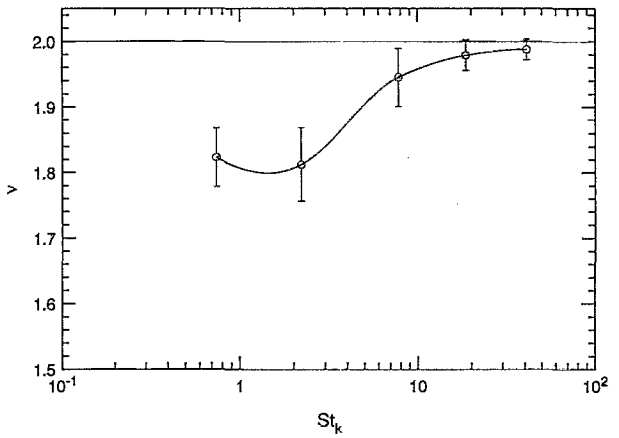

FIG. 11. Correlation dimension versus Stokes number. Smaller values of ν indicate greater preferential concentration.

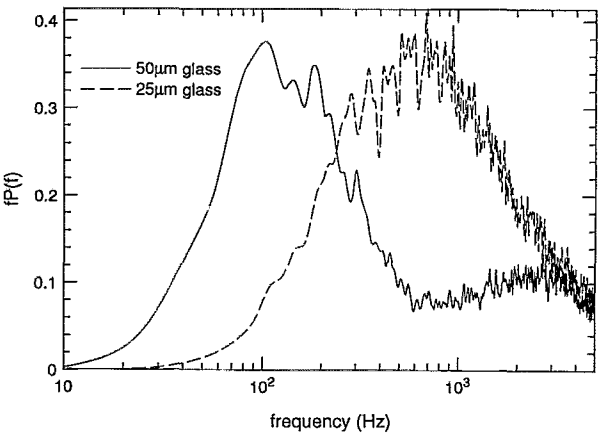

FIG. 12. Power spectrum of scattered light intensity for 25 and 50 μm glass particles.

sion, as introduced by Grassberger and Procaccia,[24] to quantify the degree of preferential concentration in mixing layer and plane wake flows. We have computed the correlation dimension similarly for this flow. The technique involves choosing a base particle and counting the number of particles that are within a certain distance l of that base particle. If the particles are uniformly distributed throughout the plane, the number of particles within a circle of radius l centered on the base particle, $N(l)$, will scale with the area of the circle (l^2) while if the particles are concentrated into a line $N(l)$ will scale linearly with l. The correlation dimension, ν, is then defined as simply the slope of $\mathrm{Log}(N(l))$ vs $\mathrm{Log}(l/L_0)$ where L_0 is some suitably defined reference length. The value of ν will be bounded by 2 for perfectly uniformly distributed particles and by 1 for particles organized into a line. Minimum correlation dimension should therefore reflect maximum organization of the particles into clusters. For this study 1000 base particles were chosen randomly in each photograph and the correlation dimension was obtained for the range of scales from $l=0.3$ to 4.5 mm, corresponding to the range of scales over which preferential concentration was observed in the photographs. The correlation dimensions from all photographs for a single particle class were then averaged to produce a single parameter quantifying the preferential concentration for that particle. The results of this work are shown in Fig. 11 and the error bars represent the standard deviation of ν over the number of photographs used in the study. The results are similar to those seen in Fig. 10 which show maximal preferential concentration at Stokes numbers around one and virtually random distribution of the largest Stokes number particles. The advantage of this technique is that it provides a single quantitative measure of preferential concentration and has no dependence on the length scale used for computation as a single parameter is derived from a wide range scales.

B. Power spectrum results

Figure 12 shows the spectra for 25 and 50 μm glass particles. It is apparent from the plot that the spectrum for the 25 μm glass is shifted to higher frequencies as compared to that for 50 μm glass. This is to be expected as Fig. 8 shows the 25 μm glass to be maximally concentrated at smaller scales than the 50 μm glass and smaller scales correspond to higher frequencies. There is a peak in the spectrum for 50 μm glass between frequency values of 100 and 200 Hz. These frequencies correspond to streamwise length scales of 10 and 5 cm respectively where the mean particle velocity is used to transform from frequency to length. While these values may seem large for a channel with a half-width of 2 cm, they may represent simply the spacing between particle clusters rather than the size of the clusters. The length scale values are consistent with the photographic evidence, which shows only a single or a fraction of a structure in the 4 cm of streamwise length that is visualized. A second, broad peak of lesser magnitude is seen in the spectrum at higher frequencies around 2500 Hz. These frequencies correspond to lengths on the order of 4 mm. This peak could represent the size of the particle clusters, as information about both the size and spacing of clusters should appear in the power spectrum. In fact, the value of 4 mm is in reasonable agreement with Fig. 9, which shows 5 mm to be the box size for maximum D. The 25 μm glass on the other hand shows a single broad peak from 300 to 1000 Hz that corresponds to particle cluster spacings of 3 to 1 cm. This is also consistent with the photographic results which show several structures per photograph. No secondary peak representing the cluster size is present for the 25 μm glass particles because the signal was filtered at a frequency very close to where that peak should occur.

The cluster spacings found for the 25 and 50 μm glass particles, O (2 cm) and O (7 cm), are an order of magnitude higher than the box sizes for maximum concentration—3 mm and 7 mm, respectively. It is important to note that preferential concentration, as measured by D, will be maximum when the box size is on the order of the particle cluster size. Larger boxes will contain regions of both high and low concentration. The scale of the particle clusters does not, however, correspond to the scale of the structures which cause the clustering. Particles in flows dominated by large-scale two-dimensional vortices are collected in thin strands on the

edge of the vortices. The results of Longmire and Eaton,[8] for example, show particles concentrating in the highly strained saddle regions between sucessive vortices and the clusters are relatively small compared to the vortices in the flow. Thus the spacing between clusters is more indicative of the size of the flow structures causing the concentration than the size of the clusters. The length scales from the spectral analysis give a better representation of the spacing between the particle clusters and thus the structures in the flow than the box size for maximum D. However, both types of information, cluster size and spacing, are necessary to statistically describe the particle concentration field.

V. SUMMARY AND CONCLUSIONS

A study of the particle concentration field at the centerline of a turbulent channel flow has been conducted. As the centerline of a channel flow is a region of nearly homogeneous turbulence these results can be compared to computational results for homogeneous turbulence. Photographic images were processed digitally to produce the particle concentration field on a range of grid sizes for five different particle classes. Quantitative descriptors of the deviation of the particle concentration field from a purely random distribution show that preferential concentration of particles occurs in homogeneous flows with fully three-dimensional turbulence structure. Determining which particle is most preferentially concentrated is a complex issue, however, because different particles are found to be concentrated on different scales. This is to be expected, as each particle should be affected most by eddies which correspond to Stokes numbers on the order of one for that particular particle. Thus, one must ask not only what particle size is most preferentially concentrated but also at what scale does the concentration occur. The correlation dimension has been used to obtain a single quantity which characterizes the preferential concentration over a wide range of scales. Both of the methods of assessing preferential concentration show maximal preferential concentration occurs when the Stokes number of the particles based on the Kolmogorov time scale is of order one.

The spacing between particle clusters was also investigated for two of the particle sizes and found to be an order of magnitude larger than the box size for maximum concentration. Studies involving flows with large coherent vortices have shown that the spacing between particle clusters is a better gauge of the flow structures causing preferential concentration than the size of the clusters themselves. Although Kolmogorov scaling seems appropriate for defining a particle Stokes number in complex three-dimensional flows, the length scales of both the particle clusters and the fluid structures causing the concentration are significantly larger than Kolmogorov length scales.

ACKNOWLEDGMENTS

The authors appreciate the sponsorship of the National Science Foundation (Grant No. CTS-9005998-03). The first and second authors were also supported by National Science Foundation Graduate Fellowships during the first three years of their graduate studies. The authors would also like to thank Joe Eaton for his work on computing the correlation dimension for this study.

[1] C. T. Crowe, R. A. Gore, and T. R. Troutt, "Particle dispersion by coherent structures in free shear flows," Part. Sci. Tech. **3**, 149 (1985).
[2] J. K. Eaton and J. R. Fessler, "Preferential concentration of particles by turbulence," Int. J. Multiphase Flow **20** (Suppl.), 169 (1994).
[3] H. Kobayashi, S. M. Masutani, S. Azuhata, N. Arashi, and Y. Hishinuma, *Transport Phenomena in Turbulent Flows—Theory, Experiment, and Simulations*, edited by M. Hirata and N. Kasagi (Hemisphere, New York, 1988), pp. 433–446.
[4] F. Wen, N. Kamalu, J. N. Chung, C. T. Crowe, and T. R. Troutt, "Particle dispersion by vortex structures in plane mixing layers," J. Fluids Eng. **114**, 657 (1992).
[5] B. J. Lazaro and J. C. Lasheras, "Particle dispersion in the developing free shear layer. Part 1. Unforced flow," J. Fluid Mech. **235**, 143 (1992).
[6] B. J. Lazaro and J. C. Lasheras, "Particle dispersion in the developing free shear layer. Part 2. Forced flow," J. Fluid Mech. **235**, 179 (1992).
[7] Y. Yang, C. T. Crowe, J. N. Chung, and T. R. Troutt, "Quantitative study of particle dispersion in a bluff-body wake flow," ASME FED, Gas–Solid Flows **166**, 231 (1993).
[8] E. K. Longmire and J. K. Eaton, "Structure of a particle-laden round jet," J. Fluid Mech. **236**, 217 (1992).
[9] M. Rashidi, G. Hetsroni, and S. Banerjee, "Particle turbulence interaction in a boundary layer," Int. J. Multiphase Flow **16**, 935 (1990).
[10] J. B. Young and T. D. Hanratty, "Trapping of solid particles at a wall in a turbulent flow," AIChE J. **37**, 1529 (1991).
[11] J. W. Brooke, K. Kontomaris, T. J. Hanratty, and J. B. McLaughlin, "Turbulent deposition and trapping of aerosols at a wall," Phys. Fluids A **4**, 825 (1992).
[12] S. Pedinotti, G. Mariotti, and S. Banerjee, "Direct numerical simulation of particle behavior in the wall region of turbulent flows in horizontal channels," Int. J. Multiphase Flow **18**, 927 (1992).
[13] D. W. I. Rouson and J. K. Eaton, "Direct Lagrangian/Eulerian simulation of solid particles interacting with a turbulent channel flow," *ASME International Symposium on Numerical Methods for Multiphase Flows*, Lake Tahoe, Nevada (American Society of Mechanical Engineers, New York, 1994).
[14] M. R. Maxey, "The gravitational settling of aerosol particles inhomogeneous turbulence and random flow fields," J. Fluid Mech. **174**, 441 (1987).
[15] K. D. Squires and J. K. Eaton, "Particle response and turbulence modification in isotropic turbulence," Phys. Fluids A **2**, 1191 (1990).
[16] K. D. Squires and J. K. Eaton, "Preferential concentration of particles by turbulence," Phys. Fluids A **3**, 1169 (1991).
[17] L. Wang and M. R. Maxey, "Settling velocity and concentration distribution of heavy particles in homogeneous isotropic turbulence," J. Fluid Mech. **256**, 27 (1993).
[18] P. Neumann and H. Umhauer, "Characterization of the spatial distribution state of particles transported by a turbulent gas flow," Exp. Fluids **12**, 81 (1991).
[19] Y. Sato (personal communication, 1993).
[20] J. D. Kulick, J. R. Fessler, and J. K. Eaton, "Particle response and turbulence modification in fully-developed channel flow," J. Fluid Mech. **277**, 109 (1994).
[21] L. B. Torobin and W. H. Gauvin, "Fundamental aspects of solids–gas flow," Can. J. Chem. Eng. **37**, 129 (1959).
[22] G. R. Ruetsch and M. R. Maxey, "The evolution of small-scale structures in homogeneous turbulence," Phys. Fluids A **4**, 2747 (1992).
[23] L. Tang, F. Wen, Y. Yang, C. T. Crowe, J. N. Chung, and T. R. Troutt, "Self-organizing dispersion mechanism in a plane wake," Phys. Fluids A **4**, 2244 (1992).
[24] P. Grassberger and I. Procaccia, "Measuring the strangeness of strange attractors," Physica D **9**, 189 (1983).